STEEL STRUCTURES
www.ijoss.org
Steel Structures 8 (2008) 91-108

Parametric Study on Static Behaviour of Self-anchored Suspension Bridges

Arie Romeijn*, Reza Sarkhosh and David van Goolen

Faculty of Civil and Geosciences, Technical University of Delft, 2628 CN Delft, The Netherlands

Abstract

This study is done to develop a set of consistent design guidelines for self-anchored suspension bridges and discusses static behaviour as well as feasibility study of long span self-anchored bridges. In order to accomplish this goal, a thorough investigation of important parameters to determine behaviour of self-anchored suspension bridge and identify any gaps on current knowledge is done to be filled in order to enable the formation of a consistent set of design recommendations. This research indicated that a well-chosen ratio between the bending stiffness of deck and axial stiffness of cable influences the maximum bending moments and the deflections in the girder. The ratio of sag to span is also investigated to reduce the normal force in the deck and the maximum bending moment in the deck. A study to the static strength, stiffness, frequency behaviour and the buckling stability of the box girder, revealed that a deck slenderness of the box girder of $\lambda = 1/100$ and even more slender is very well feasible. The paper also discusses possibilities of increasing main span length and tries to find a certain span limit for the self-anchored suspension bridges. Increasing the span length of the bridge will cause several effects on static strength and stiffness. Several effects are monitored like stresses in cable, girder and pylon, deformations and reaction forces. Based on results of this study, a span length of 500 metres is very well possible and even beyond that.

Keywords: Suspension, Bridge, Self-anchored, long span, Finite element model, Parametric, Static behaviour, Feasibility study

1. Introduction

Since 1870, only about 25 highway bridges have been executed as a self-anchored suspension bridge. The rise of the cable stayed bridge since 1955 made this suspension type an obsolete alternative for a long period. The largest ever built self-anchored suspension bridge is the Cologne-Mulheim Bridge with a main span of 315 m in Germany (1929). As it no longer exists today, both Konohana (Japan 1990) and Yeongjong Grand Bridge (Korea 1999) have the largest main span (300 m) at present day. The East Bay Bridge near San Francisco with a main span of 385 m will surpass this record and will become the largest self-anchored suspension bridge ever. Main difficulties for this bridge type to reach spans over 300 metres can be blamed on erection problems and the buckling stability of the girder. Erecting the deck structure prior to the main cable makes this bridge technically and economically less attractive than for instance the cable stayed bridge.

This manuscript for this paper was submitted for review and possible publication on February 27, 2008; approved on June 12, 2008.

*Corresponding author
Tel: +31-15-278 3705; Fax: +31-15-278 3173
E-mail: A.Romeijn@tudelft.nl

The principle of a self-anchored suspension bridge is that it carries the horizontal component of the main cable tensile force to the bridge deck structure. This results in a considerable compression force in the bridge deck making it prone to global buckling risks of the bridge deck. Only a vertical component of the cable tensile force is still to be resisted. Therefore, the deck resists the horizontal component of the cable force and also carries the vertical traffic loads and spreads through the many hangers to the suspension cable. Compression force in the deck results to a stiffer deck compare with conventional suspension bridges. This makes a better sense when looking at the span length to width ratio for the classic concept that varies around 40 and for the self-anchored that this ratio is around 10.

A similar comparison can be made for deck slenderness and sag to span ratio. In self-anchored bridges there is lower girder slenderness. This is related to the problem of global buckling stability of the deck and so requires a stiffer girder. To achieve this, the depth of girder is enlarged. The span to girder height ratio in self-anchored bridges is between 20 and 120 whiles this ratio is between 100 and 600 in conventional suspension bridges. The axial force in the stiffening girder of self-anchored suspension bridges is contrary to the sag to span ratio, thus so far forth as the sag to span ratio is larger, the axial force becomes lower. Larger sag to span ratio results in a

lower horizontal cable force, which is favourable with respect to the global buckling stability of the stiffening girder in the self-anchored type. The sag over span ratio of conventional suspension bridges are about 1/10 while recent self-anchored bridges show a sag to span ratio between 1/5 and 1/8. The self-anchored suspension bridge is comparable to a cable stayed bridge in a way that it also is anchored in itself to resist the horizontal components of the cables. The second similar system is found in the tied arch. The bridge deck of a tied arch resist the horizontal component of the compression arch leaving a tensile force in the bridge deck.

The objective of this research is to study the static behaviour of a self-anchored suspension bridge as well as feasibility study of a long span suspension bridge. A reference model is designed and used to investigate the influence of several parameters on static behaviour of a self-anchored suspension bridge. This model is submitted as part of a feasibility study for a suspension bridge to cross over the Waal River (Fig. 1) in Nijmegen city, the Netherlands.

The reference design is modelled in a finite element program to investigate and calculate the force distribution and deformations. With help of the reference design, a complete study on main design criteria like static strength, stiffness and the buckling stability of the girder is done. First results are given of a parameter. The results of the parameter study are used to determine an optimization of the reference design. Finally, to identify the influence of increasing span length and find a certain span limit for the self-anchored suspension bridge, further study is done.

2. Reference Design

The total width of the Waal River and riverbanks is succeeding 1000m and the average width of the river is 325 m. Horizontal navigation clearance of 265 m and Vertical of 9.10m are requested to be considered in design of the suspension bridge.

The total length of the bridge is 375 m and the main suspended span is 150 m. As shown in Fig. 3, the bridge has two 11.70 m wide carriageways, separated by a 0.60m wide central separator, and two 5.80 m pedestrian and cyclist lanes, including two 0.60 m separator and railing in each side (Overall width of 35.60 m). Van Goolen (2007) has described all details about the bridge and Waal River.

A main span length of 150 m and two 62.50 m side spans length with several approach spans are chosen as a starting point for the so-called reference model. With this chosen main span of 150 m it is possible to investigate later on the influence of an increasing span length to about 500 m on the mechanical properties of the stiffening girder. For the configuration of the main cable, a parabolic shape is chosen. In reality, a cable has a catenary shape when it is loaded by its self-weight (Fig. 4). The catenary shape is well approximated with a

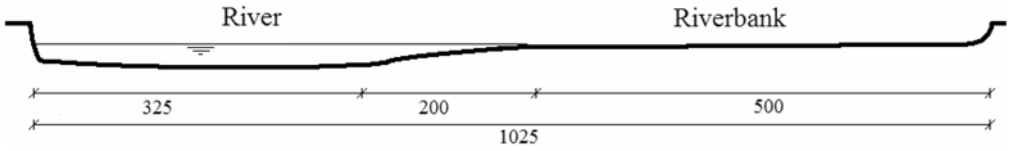

Figure 1. Waal River cross section.

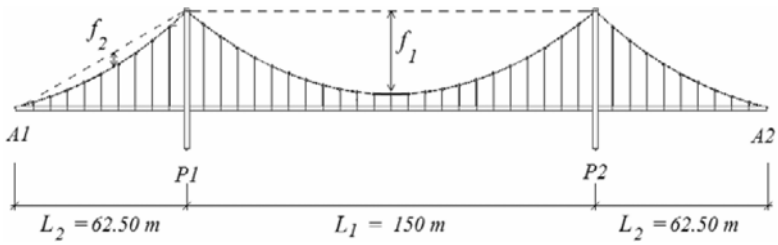

Figure 2. Schematic elevation of bridge.

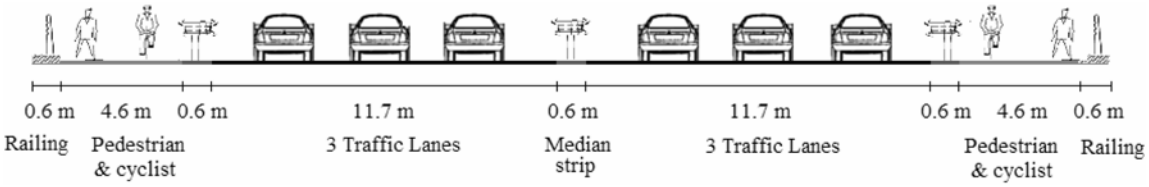

Figure 3. Bridge traffic lanes and railing.

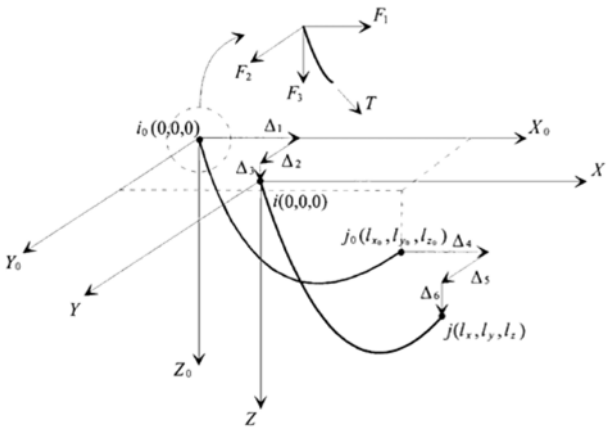

Figure 4. Three-dimensional elastic catenary cable element (Kim *et al*., 2002).

parabolic line. Therefore, a parabolic shape is assumed for the main cable in main and side span. The sag of the cable in the mid of the side span (f_2) is determined by Ulstrup (1993):

$$f_2 = f_1 \times \frac{L_2^2}{L_1^2} \quad (1)$$

where, f_1 and f_2 are the main cable sag in main span and side spans respectively, L_1 is the main span length and L_2 is the side span length.

Fig. 2 shows a schematic representation of the bridge. The bridge deck is a steel box girder consisting of longitudinal and transverse stiffeners, cross beams and diaphragms (Fig. 5). For structural elements like deck and pylon, a steel grade S355 is used with Yield strength of $f_y = 355$ N/mm^2 and modulus of Elasticity of $E = 21000$ N/mm^2. For pylons, a standard H-frame is chosen with a steel box cross section. For the main cable and hangers, parallel steel round wires with tensile strength of $f_y = 1770$ N/mm^2 is used.

For the mid of the main span, a maximum allowable design stress of 200 N/mm^2 is chosen for pre-design purposes. After calculation of several bridge components and optimization of the reference design, the bridge dimensions and mechanical properties are presented in Table 1. It has to be mentioned that some dimensions like stiffeners or additional plates are eliminated in this table.

Table 1. General properties of the bridge (equivalent)

Girder	top flange thickness	40 mm
	bottom flange thickness	20 mm
	web thickness	15 mm
	height	2100 mm
	width	35600 mm
Main cable diameter		160 mm
Hangers diameter		55 mm
Pylon	width	2000 mm
	depth	2000 mm
	thickness	25 mm
	Total height	50000 mm

3. FE modelling

Finite element modelling is done using SCIA ESA-PT software (2006). This program enables the designer to model a structure and to apply certain loads and loading combinations from which the effects like member forces and deflections can be calculated.

With beam elements, the 3D model is built up with one dimensional line elements. This enables to model the total bridge structure and calculate member forces due to certain load cases and combinations.

The scope of the model is to be able to analyse the model statically in a three dimensional way. Also an assessment will be made with respect to the geometric non linear effects of a cable supported bridge, the so-called second order effects. Fig. 6 shows the FE-model of the bridge.

3.1. Pylon

The pylon is modelled as a simple portal frame. The

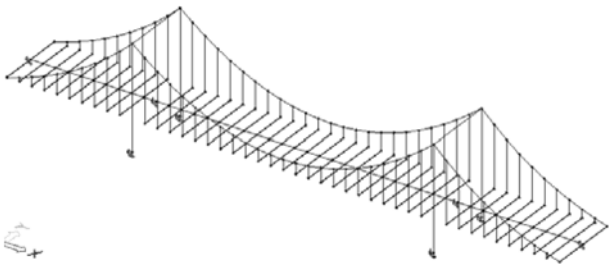

Figure 6. FE model of the bridge with beam elements.

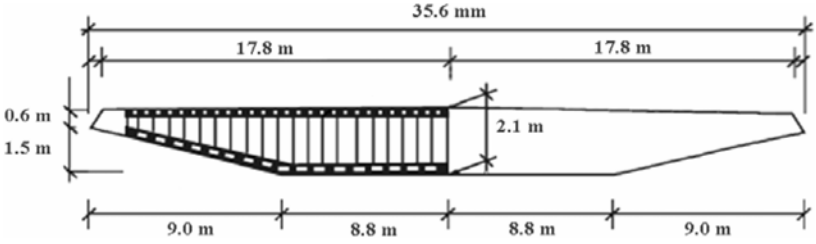

Figure 5. Cross section of the deck (Reference design).

cross section consists of a steel box. At the basement, the pylon is rotationally fixed to provide for longitudinal stiffness to structure. An axial compression force and a bending moment due to horizontal force on the pylon caused by the tensile force in the main cables load the pylon.

The pylon is fixed supported in transverse and longitudinal direction of the bridge. For ease of modelling, the deck, represented by the stiffening girder, is vertically supported on the 'outside world' at the pylon. One rotation fixed support creates the effect of two supports on the stiffening girder. Modelling the pylon and bridge deck this way, cancels out any influence of the girder support on the pylon. This is assumed negligible.

3.2. Main cable

The main cable is modelled with cable elements, which are beam elements with a very low bending stiffness. In addition, no shear forces exist for the cable. The cable element is subjected to its own weight and accounts for the slackening effects in cables under self-weight load. Another effect of a cable element, which can be distinguished, is that the slack causes a tension in the cable and therefore a horizontal reaction on the supports.

For modelling of the cable, an equivalent modulus of elasticity has to be used to account for elastic stretch and lengthening of the cable due to geometry change. These two effects reduce the modulus of elasticity. The equivalent modulus of elasticity can be determined using the formulae developed by H.J. Ernst (1965). Euro code EN-1993-1-11 states for the effective modulus of elasticity:

$$E_t = \frac{E}{1 + \frac{w^2 l^2 E}{12\sigma^3}} \tag{2}$$

which E is the modulus of elasticity of the cable, w is the unit weight, l is the horizontal span of the cable and σ is the stress in the cable due to self weight and permanent loading. For the reference model, a bunch of parallel wires is chosen.

3.3. Hanger cables

For hangers, parallel strands with the same cable type as main cable is chosen. A cable fabricated with a bundle of parallel strands has the largest modulus of elasticity compared to other cable types and is therefore chosen. Also for increasing span lengths, it becomes impossible to apply prefabricated locked coil.

3.4. Stiffening girder

A single beam element is used to model the stiffening girder. In that way, the mechanical properties can easily be adopted. The girder is located in the middle of the two cable planes and is connected to hangers by means of 'rigid arms'.

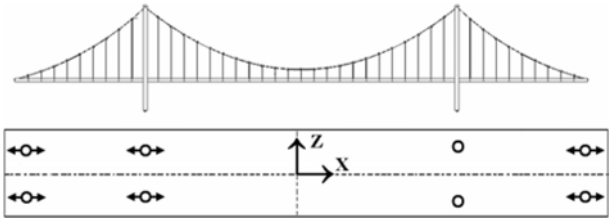

Fig. 7. Bearing System

A rigid arm is a connection between nodes with infinite stiffness, which transfers all deformations from one node to the other node. The rigid connection between the cable plane and the stiffening girder transfers the deformation of the cable and hangers to the stiffening girder.

3.5. Supports

Along the length of the bridge, the girder is vertically supported on four locations: end supports and at the pylons. All the supports are vertically fixed and rotation fixed around the longitudinal direction of the bridge deck to create a support reaction similar to a system of two supports.

The stiffening girder is vertically supported on bearings at the pylon. Transverse direction of the girder is fixed and longitudinal direction is also fixed at Pier 2 (Fig. 7).

3.6. Loads

For analysing the static behaviour and exploring the span possibilities, only the main loads are taken into account. These are vertical loadings such as dead loads and live loads based on Eurocode. Dead loads (self weight of the steel girder and cables with $\gamma_{steel} = 78.5$ kN/m^3), uniform distributed traffic loads (highway traffic, pedestrian, bicycles) and concentrated axle loads are applied to the girder.

To apply the traffic loads, it is translated to a resulting line load which acts as a distributed line load along the longitudinal direction of the stiffening girder. Because of the asymmetry of the traffic loads, the resulting line load has a certain eccentricity to the gravity centre of the box girder ($e = 1480$ mm) and a value of $q_{res,traffic} = 131.50$ kN/m.

In addition, the axle three loads are reduced to a resulting concentrated load $F_{res} = 600 + 400 + 200 = 1200$ kN with an eccentricity of 7.7m. For pre-design reasons the concentrated loads are left out of consideration because their global influence is not significant. For local design of the orthotropic deck, it becomes important to consider these local loading conditions for design of longitudinal and transverse stiffeners.

Three load cases (traffic over the entire length of the bridge, on the side span only and on the mid span only) in combination with self-weight, permanent loading and pre-tensioning of the main cable are considered in this parametric study. The suspension bridge is modelled according to its final desired geometry under self-weight. In many cases, the main cable is given a pretension so

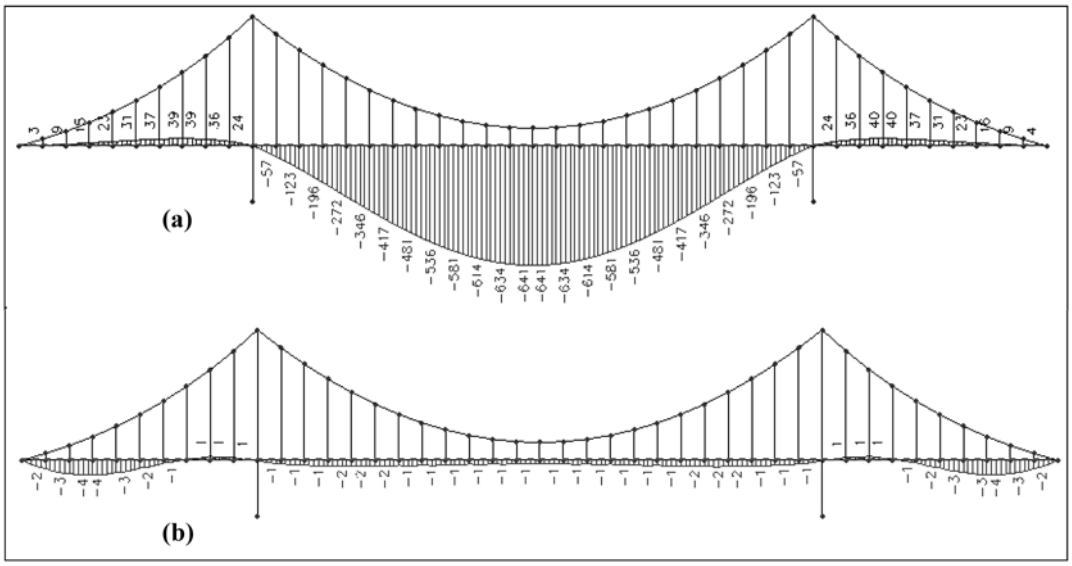

Figure 8. (a) Deflection of girder (mm) due to self weight only. (b) Deflection of girder (mm) due to self weight after pretensioning the main cable.

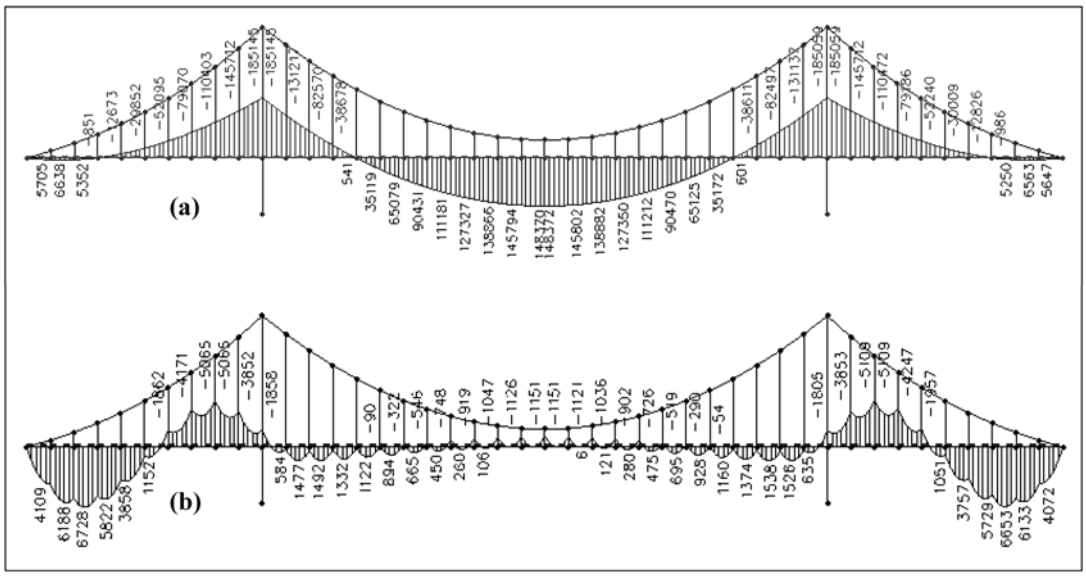

Figure 9. (a) Deflection global bending moments (kN-m) in girder due to self weight. (b) Bending moments (kN-m) in girder due to self-weight after pretensioning main cable.

that under dead load the bridge adopt it final desired shape. Therefore, the ideal FE model of a suspension bridge should represent a situation that on application of the self-weight load, the geometry of the bridge does not deviate from the desired final shape of the bridge (Ren, 2004).

Furthermore, a general assumption in suspension bridge design is to have a reduced global bending moment to about zero under self-weight loading. This means that one wants to achieve that the self-weight load is completely supported by the main cable. This can be approximately achieved by manipulating the initial tensile force in de the main cable. The initial tensile force in the main cable can be found by trial and error until a situation is created with minimum deck deflection and minimum bending stresses caused by the global bending moment in the stiffening girder.

In the FEM program this initial tensile force on the main cable is done by applying a temperature load that causes the cable to become shorter which is just a modelling tool to apply a pretension on a structural member. Fig. 8(a) shows the deflection due to self weight only (deflection in mm). When the main cable is given a certain amount of pretensioning (determined iteratively), the deflection of the girder is reduced to nearly zero, see Fig. 8(b).

Moreover, the bending moments reduce to nearly zero. Fig. 9(a) shows the bending moment distribution due to

self weight only and Fig. 9(b) shows the bending moments after pretensioning of the main cable. Fig. 9(b) clearly shows the reduced global bending moment to zero and the resulting small local bending moment between the hangers.

Because the global bending moment is reduced to nearly zero, the assumption that the bending stresses in the girder are almost reduced to zero under self-weight loading, is hereby verified.

4. Stability of the Girder

A stability check is done for the stiffening girder because it is loaded with a large axial compression force. A stiffening girder under compression is prone to global buckling effects. To make an assessment of the buckling risk of the girder, the Euler buckling force is determined.

An indication for the stability of the bridge deck is the occurrence of second order effects regarding the deflections of the bridge deck. A second order analyses is performed because in cable supported structures geometrical nonlinearity can be of importance. In general, long span bridges such as cable stayed- and suspension bridges exhibits geometric nonlinearity due to:

- The combination of axial compression forces and bending moments, which act in the stiffening girder and the pylon.
- The nonlinear behaviour caused by the cable. The relation between forces and the resulting deformations are not linear. (e.g. an increased self weight load in the cable results in a reduction of live load deflection (Gasparini- 2002, Gimsing-1998). The tensile force in the cable produces a geometrically non-linear stiffness of the cable)
- Geometry changes in the bridge structure caused by large displacements.

At first sight, the reference model revealed hardly any second order effects. There is no amplification of the deflection of the stiffening girder visible in the second order analyses under the given loading conditions. Fig. 10 shows that for the three considered load combinations the second order effects are hardly visible. This indicates that the reference bridge model behaves very stiff and that the deflections are relatively low to cause major second order effects. Causes for the hardly visible second order effects could be that:

- The combination of axial forces and bending moments that act in the stiffening girder and the pylon are not significant enough to cause visible second order effects in the deflection of the stiffening girder. This reference model showed normal stresses in the deck, caused by the deck compression force, of about 15 N/mm^2. This is relatively low.
- The stiffening effect of the girder. The illustration that is presented in Fig. 11 indicates that regarding the reference model with a main span of 150 metres,

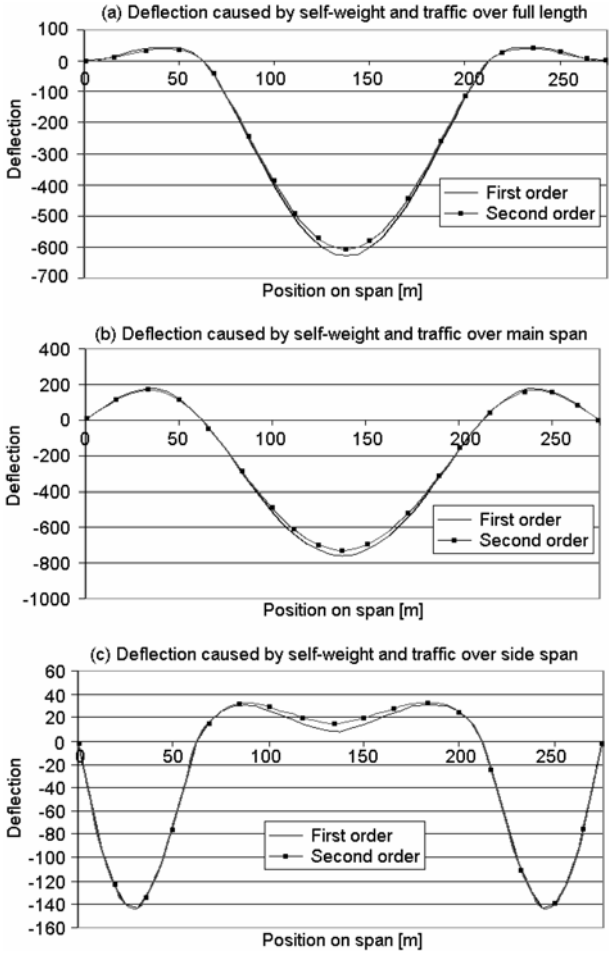

Figure 10. 1st and 2nd order deflection due to the three considered loading combinations including pretension of main cable.

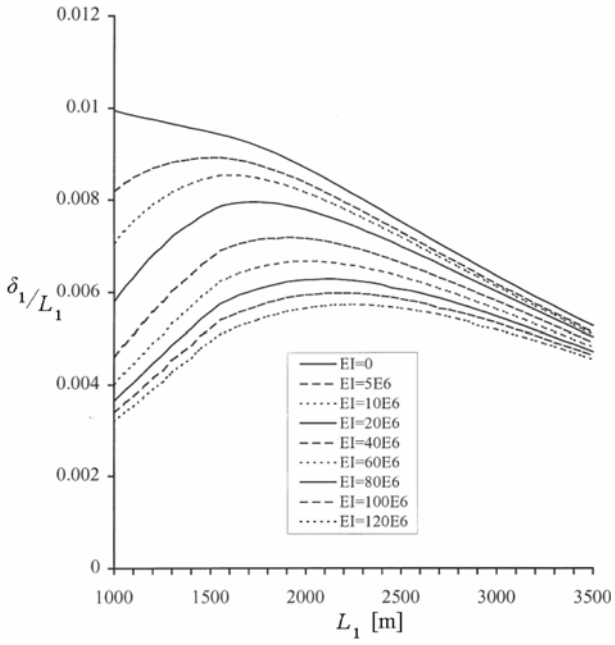

Figure 11. Decreasing stiffening effect (Clemente *et al.*)

the stiffening effect of the bridge's main girder is significantly large. Fig. 11 shows the relation between the non-dimensional maximum deflection δ_1/L_1 against L_1 (δ_1 = deflection and L_1 = main span length). For different values of the girder bending stiffness EI_{Girder}, a decreasing influence on displacement is visible when the main span (>2000 metres) is increased.

For main span smaller than 2000 metres, Fig. 11 indicates that the stiffness of the girder has a significant effect on the reduction of the deflection in the bridge. For a main span of 150 metres this would indicate that the stiffness of the deck has large influence on the reduction of the deflections of the total bridge structure. And therefore large geometry changes (which is in many cases a cause for geometric non linear behaviour) in the bridge structure caused by large displacements are not expected to exhibit in relatively small spans like 150 metres of the reference model.

So the combination of the relatively small deflections and stiff behaviour of the girder are causes for the hardly visible second order effect for the reference model in this study. To determine the buckling force, an additional normal force is imposed on the stiffening girder of the reference model of the bridge, which helps second order effects do become visible. Application of additional normal force on the girder is described in section 5.1.

In this case an additional force of $\Delta F = 400000$ kN is applied, about ten times the design value of the normal force in the deck (N). Now an assessment of the Euler buckling force can be made with respect to the three considered load cases. A distinction is made between the main and the side spans because the amplification of the deflections deviates from each other. From this distinction the decisive Euler buckling force can be retrieved, the smallest buckling force to cause buckling in the either the main span or the side span is the governing one. For the reference model, the design value of the normal force is N, depends on loading combination as presented in Tables 2-4.

Table 2. Euler buckling force with traffic over full length

	δ_1 (mm)	δ_2 (mm)	n-value	$N_{cr} = n \cdot N$ (kN)
Main span	790	1608	1.97	851867
Side span	48	236	1.26	544849

Table 3. Euler buckling force with traffic over main span

	δ_1 (mm)	δ_2 (mm)	n-value	$N_{cr} = n \cdot N$ (kN)
Main span	883	1882	1.88	813145
Side span	129	407	1.46	631485

Table 4. Euler buckling force with traffic over side span

	δ_1 (mm)	δ_2 (mm)	n-value	$N_{cr} = n \cdot N$ (kN)
Main span	155	217	3.50	1481603
Side span	84	112	4.00	1693260

The stability check according to the Eurocode3:

$$\frac{N}{\frac{\chi N_{cr}}{\gamma_{M1}}} + \frac{\beta_m (M_{Y,deck} + \Delta M_Y)}{\frac{M_{Y,rk}}{\gamma_{M1}}} \leq 0.9 \quad (3)$$

$$\frac{N}{\chi N_{cr}} + \frac{\beta_m M_{Y,deck}}{M_{Y,Rk}} = 0.477 \leq 0.9 \quad (4)$$

In which, $N = 32420$ kN, $N_{cr} = 544849$ kN, $\chi = 0.484$, $\beta_m = 1.27$, ΔM_Y = not applicable because the entire cross section is assumed to resist the acting normal force in the cross section of the box girder. $\gamma_{M1} = 1$, $M_{y,RK}$ is the critical moment in side span.

Overall conclusion is that the bridge girder satisfies the stability check according the Eurocode check. Therefore, the conclusion can be made that the stiffening girder in the reference model is stable against buckling.

5. Parameter Study Into Static Behaviour

To study the effect and sensitivity of the mechanical properties of girder, pylon and cable on the bridge's behaviour, several parameters been checked, like EI_{Girder}, EI_{Pylon}, EA_{Cable} and sag to span ratio. The influence of these parameters on global stiffness, reaction forces, bending moments and stability of the girder has been checked. Results are analysed and presented in tables and graphs to visualize the effects. Results of the parameter study are presented in graphs, which illustrate the developments of:

- Bending moments in girder at support and main span
- Deflection of pylon and girder at mid span
- Frequencies, 1st bending and 1st torsional frequency
- Ratio of bending moment carried by deck and cable

5.1. Influence of girder height

In order to investigate the influence of various bending stiffness and torsional stiffness on structural behaviour of the bridge, the height of the box girder is chosen varied from 1/50 up to 1/100 of the length of main span. A slenderness of 1/50 means a structural height of 3.0 m and 1/100 a height of 1.5 m. Table 5 shows the girder height with corresponding flexural stiffness and torsional stiffness. This table is also presents the influence of the girder height on several parameters like main cable force (H), vertical displacement of the girder at mid span (δ_{main}), longitudinal displacement of the pylon at top (δ_{pylon}) and total moment in girder at mid span with contribution of deck and main cables ($M_{Y,total}$).

Increasing the bending stiffness has a significant effect on the moment distribution. A larger stiffness of the girder means the bending moments increase significantly, with approximately 95%.

Fig. 12 clearly shows that with an increasing stiffness, the girder tends to carry a larger part of total bending moment and smaller participating by the main cable, leads to reduce the normal force. The total bending

Table 5. Influence of the properties of the girder on bridge behaviour

Height (mm)	I_y (m^4)	I_t (m^4)	N (kN)	H (kN)	R_z (kN)	δ_{main} (mm)	δ_{pylon} (mm)	$M_{Y\,total}$ (kN-m)	$M_{Y\,support}$ (kN-m)	1^{st} *bending freq.* (Hz)	2^{nd} *bending freq.* (Hz)	1^{st} *torsional freq.* (Hz)	2^{nd} *torsional freq.* (Hz)
1500	1.1085	2.78139	35502	18159	6975	474	120	104641	137291	0.63	1.10	4.58	3.97
1700	1.4213	3.54602	34388	17576	6673	433	110	121618	157416	0.67	1.23	4.83	4.07
1900	1.7735	4.39681	33359	17036	6392	395	100	137455	176048	0.70	1.35	5.04	4.14
2100*	2.1651	5.33188	32420	16542	6134	361	91	152065	193096	0.74	1.46	5.20	4.19
2300	2.5964	6.34938	31568	16094	5899	330	83	165448	208572	0.77	1.58	5.37	4.23
2500	3.0674	7.44755	30801	15690	5685	302	76	177658	222556	0.81	1.68	5.49	4.26
2800	3.849	9.24224	29793	15158	5401	265	67	193962	240982	0.86	1.83	5.63	4.29
3000	4.4203	10.5346	29206	14849	5234	244	61	203631	251751	0.89	1.92	5.71	4.31

*Properties of reference design

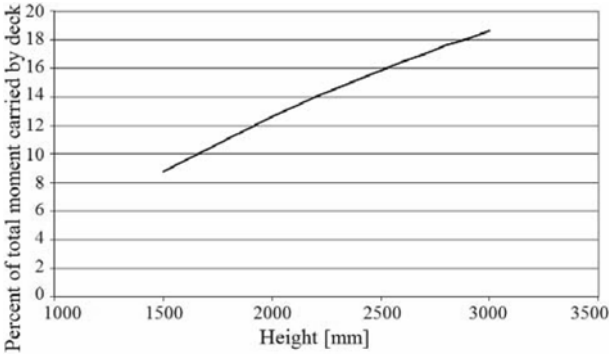

Figure 12. Moment contribution between the girder and main cable.

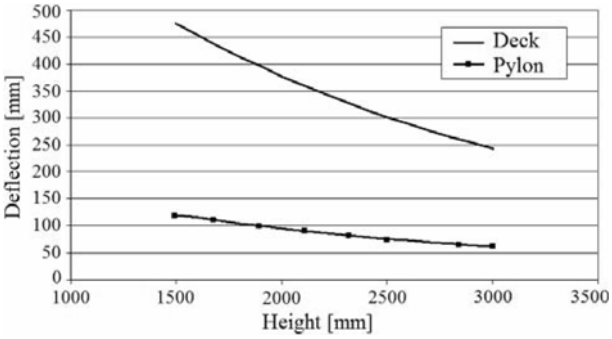

Figure 13. Maximum deflection in the girder and pylon.

moment in the main span is determined by:

$$M_{Y,total} = 2\ (H_{main\ cable} \times f_1) + M_{Y,deck} \qquad (5)$$

where, $H_{main\ cable}$ is the axial force in main cable, f_1 is the cable sag in main span and $M_{Y,deck}$ is the design value of the maximum moment about the Y axis of the member calculated with first order analyses.

An increasing stiffness of the girder result in larger global stiffness, because the deflection reduces significantly. Fig. 13 shows this tendency of a decreasing deflection of the girder and displacement of the pylon. Girder and pylon deflections are reduced with approximately 50%. An increasing global stiffness also results in higher bending and torsional frequencies. The stiffness of the

Figure 14. Additional normal force applied on the girder.

Figure 15. Spring supported bridge deck.

girder has a clear visible influence on the stiffness, strength and frequency of the bridge. The resistance of the main girder against buckling is mainly determined by the bending stiffness (*EI*) of box girder. Two approaches will be set out in this part in order to compare and verify the results of the calculation of Euler buckling force for the stiffening girder.

First approach is that on the bridge deck an additional normal force is applied to be able to analyze the second order deflections and determine the buckling force (Fig. 14). The bridge model proved very stiff and second order effects only became visible by increasing the normal force on the deck; in this case by applying an external additional force (ΔF).

The second approach is to model the main girder as a continuous girder with discrete spring supports (Fig. 15). The springs act like hangers and each one has a certain stiffness k (N/m). This model is used to analyze the buckling effect of the main span. In a real model, all hangers are pre-tensioned, and caused by an upward deformed shape the hangers are still under tensile although to a much smaller extend. That means they still function as a spring support in case of buckling. However, for a suspension bridge, the global shape of vertical displacement of the deck is that large that the hangers will not always act as an effective spring support. So for this model, the spring stiffness for an upward deflection is chosen equal to zero. The girder is also loaded by a normal force (N), similar to acting normal force in the reference design; N = 32420 kN.

According to Engesser's formula (1889), the Euler buckling force for a girder supported by springs depends

on the spring stiffness (in this case the springs represent the hangers on which the girder is supported) and the bending stiffness of the girder:

$$N_{cr} = 2\sqrt{cEI} \tag{6}$$

where, c is a bedding constant equal to the spring stiffness divided by the individual distance between the springs (in this case the c.t.c. distance between the hangers).

A spring stiffness k is chosen for the springs that result in similar deflections of the spring supported girder, under full-length traffic loading of the main span. In case of an upward deflection of the side span, the hangers will not resist the girder; therefore, the spring stiffness k is equal to zero.

A stability check is done for the stiffening girder because it is loaded with a large axial compression force. A stiffening girder under compression is prone to global buckling effects. To assess the buckling risk of the girder, the Euler buckling force is determined;

$$N_{cr} = n \cdot N \tag{7}$$

where, N is the design value of compression force and n is the amplification determined from deflection in the first order (linear) and second order (geometric non-linear) analysis of the bridge model;

$$n = \frac{\delta_2}{\delta_2 - \delta_1} \tag{8}$$

in which δ_2 is the deflection determined by a second order analyses (geometric nonlinear) and δ_1 is the deflection determined by a first order analyses (linear). The n-value represents a value that indicates the risk for global buckling of the bridge deck.

Fig. 16 presents a graph of the relation between the Euler buckling force for the main span of the bridge deck and the stiffness of the deck (moment of inertia of the box girder ranging from a girder height of 1500-3000 mm, representing a range of deck slenderness λ from 1/100 to 1/50) regarding the two models. The deck slenderness is

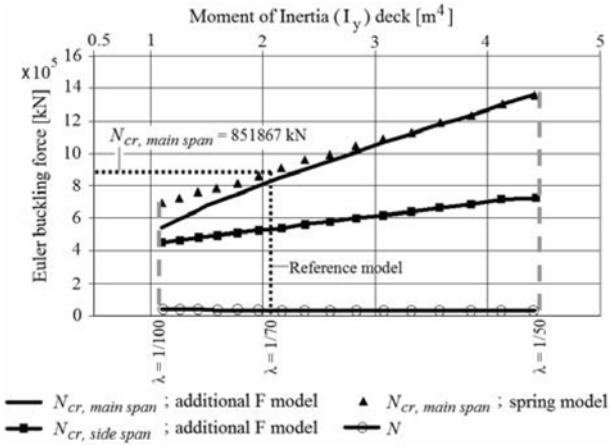

Figure 16. Euler buckling force as a function of the stiffness.

Table 6. The n-values for main and side span related to the moment of inertia of the box girder

I_y (m^4)	n-value main span	n-value side span
1.1085	15.2	12.7
1.4213	18.9	13.9
1.7735	22.4	15.3
2.17*	26.2	16.3
2.5964	30.2	18.4
3.0674	34.5	20.1
3.849	41.5	22.9
4.4203	46.6	24.9

*Properties of reference design

defined as $\lambda = h/L_1$ in which h is construction depth of the girder and L_1 is main span length. In addition, the buckling force of the side span is plotted in the graph, which is governing over the buckling force of the main span.

Both approaches display a similar development with respect to the Euler buckling force of the main span of the stiffening girder. The Euler buckling is in all cases well above the acting normal force in the deck N. Therefore in case of a more slender deck with a slenderness λ = 1/100, the resistance against buckling is still significant. The buckling behaviour of the main and side span presented in Fig. 16 can also be expressed in the n-values for main and side span based on the computed bridge model (Table 6).

These n-values also clearly show that the side span exhibits more geometrical non-linear effect, indicating that the side span is decisive for the buckling stability of the stiffening girder and that the geometrical non-linearity's decrease for both the main and the side span when the stiffness of the deck is increasing.

It can be seen in Table 5 that with increasing the girder height, the normal force in the deck and vertical reaction at the end support, both decrease. With a stiffer deck, the girder carries a larger part of the bending moment. This leads to decrease the normal force in the cable.

5.2. Influence of main cable axial stiffness

Axial stiffness (EA) of the main cable is determined by two factors; the modulus of elasticity (E) that changes with the different cable types, and the cross sectional area (A_{cable}) of the cable.

The influence of the hangers is left out of consideration in this part of the research, it is assumed to have little influence on the global strength and stiffness of the bridge.

Table 7 shows the influence of modulus of elasticity of main cable on bridge behaviour. In this table, it is clearly visible that a lower axial stiffness of the cable means that larger bending moments will act in the girder. Fig 17 shows the girder carries a larger part of the total bending moment when the axial stiffness of the main cable is reduced.

Table 7. Influence of modulus of elasticity of cable on bridge behaviour

E_{cable} (N/mm^2)	N (kN)	H (kN)	R_z (kN)	$\delta_{main\ span}$ (mm)	δ_{pylon} (mm)	$M_{Y\ totoal}$ (kN-m)	$M_{Y\ support}$ (kN-m)	1^{st} *bending freq.* (Hz)	2^{nd} *bending freq.* (Hz)	1^{st} *torsional freq.* (Hz)	2^{nd} *torsional freq.* (Hz)
205000	32420	16542	6134	361	91	152065	193096	0.74	1.46	5.20	4.19
190000	31226	15977	5763	372	94	166998	211426	0.73	1.46	5.15	4.10
150000	27504	14219	4609	408	101	213485	268570	0.70	1.46	4.93	3.83
140000	26425	13711	4275	418	104	226931	285121	0.69	1.46	4.87	3.76

*Properties of reference design

Table 8. Influence of main cable cross section on bridge behaviour

A_{cable} (mm^2)	N (kN)	H (kN)	R_z (kN)	$\delta_{main\ span}$ (mm)	δ_{pylon} (mm)	$M_{Y\ totoal}$ (kN-m)	$M_{Y\ support}$ (kN-m)	1^{st} *bending freq.* (Hz)	2^{nd} *bending freq.* (Hz)	1^{st} *torsional freq.* (Hz)	2^{nd} *torsional freq.* (Hz)
7854	18125	9806	1746	498	119	324316	408532	0.65	1.48	4.53	3.59
15394	28174	14533	4826	401	100	203917	256745	0.71	1.47	5.11	4.05
20106	32420	16542	6134	361	91	152065	193096	0.74	1.46	5.20	4.19
25447	36116	18299	7274	326	83	107047	137987	0.77	1.46	5.25	4.26
31416	39307	19822	8259	296	75	68391	90785	0.80	1.45	5.15	4.27
38013	42056	21139	9105	270	70	35380	50556	0.82	1.45	5.03	4.22

*Properties of reference design

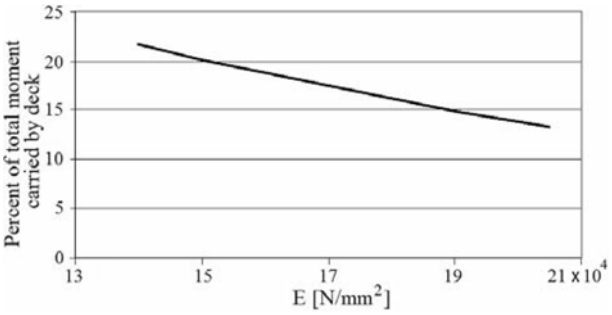

Figure 17. Moment contribution between the girder and main cable.

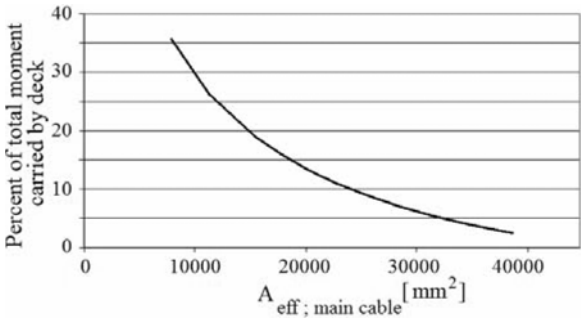

Figure 18. Contribution of the girder to bending moment.

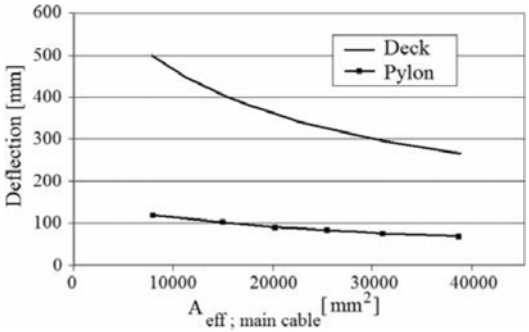

Figure 19. Maximum deflection in the girder and pylon.

A similar table is presented for the influence of main cable cross section on static parameters of the bridge (Table 8). Once a cable type is chosen, the axial stiffness of the main cable can be altered by means of the cross sectional area (A_{cable}). Increasing the diameter of the cable displays significant effects on the maximum bending moment in girder. Increasing the diameter from 160 mm to 240 mm, the bending moment in the deck ($M_{Y\ totoal}$) reduces to tenth of primary value. This means that the main cable carries nearly 100% of the total moment, which is clearly visible in Fig. 18.

Increasing the axial stiffness of the cable has favourable effects for the global stiffness; the girder deflection ($\delta_{main\ span}$) and pylon deflection (δ_{pylon}) both reduce (Fig. 19). With respect to the frequency behaviour, the increasing stiffness results in higher frequencies. Although an increment of the cable results in a decreasing torsional frequency. The reason for this can be that the self-weight of the cable rules out the stiffening effect of the cable.

A larger contribution of the main cable to the total bending moment leads to much higher reaction forces. The normal force in the deck (N) and the vertical reaction force (R_z) increase significantly.

5.3. Influence of sagging

The most common sag to span ratio for self-anchored suspension bridges are 1/5 to 1/9. In this section, it is tried to investigate the influence of several sag to span ratios on bridge behaviour.

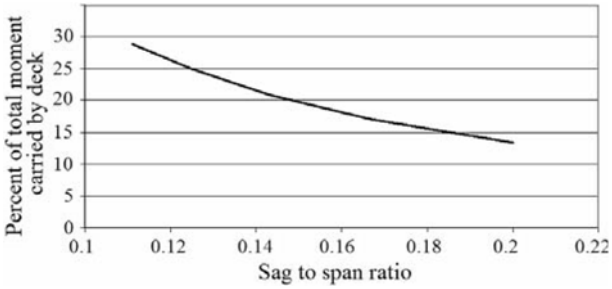

Figure 20. Moment contribution between the girder and main cable.

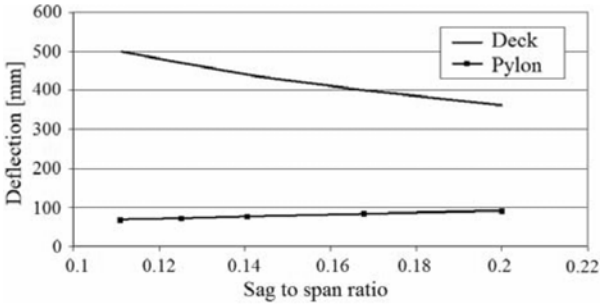

Figure 21. Maximum deflection in the girder.

In Table 9, static parameters infected by increasing sag to span ratio are presented. One of these infected parameters is bending moment. It is visible that when the sag to span ratio is in the maximum level, the cable carries a larger part of the total bending moment. With increasing sag to span ratio, the bending moment in girder reduces approximately 50%.

A larger ratio of sag to span increases the stiffness of the bridge and the decreases the main span deflection about 28%. But the deflection of the pylon increases because the height of the pylon increases with a larger sag ratio. So with an unchanged bending stiffness of the pylon, its deflection will increase when the height is increased (Fig. 21).

The first torsional frequency motion is coupled with a longitudinal deflection of the pylon; therefore, the pylon's stiffness will have effect on the torsional stiffness of the bridge. A larger sag ratio means that the pylon becomes more flexible, so a larger sag ratio decreases the torsional stiffness of the bridge, which is visible in Table 9.

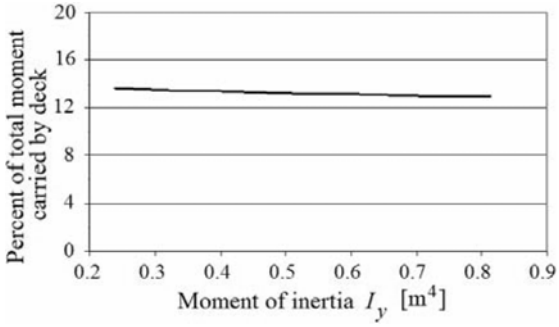

Figure 22. Moment contribution between the girder and the main cable.

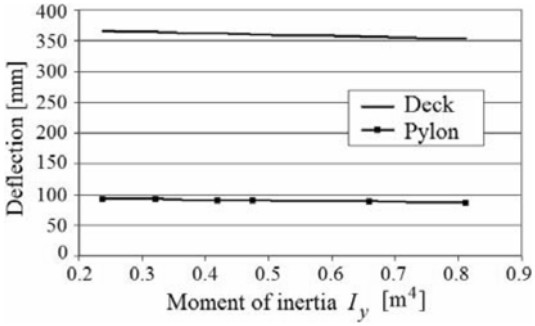

Figure 23. Maximum deflection in the girder.

Regarding the reaction forces, a larger sag ratio decreases the contribution of the cable to the total bending moment. The normal force in the main cable decreases with a larger sag ratio and so does the compression in force in the girder. Only the vertical reaction force at the end support increases because the vertical component of the normal force in main cable increases with a larger pylon height.

5.4. Influence of pylon stiffness

The influence of the bending stiffness of the pylon in longitudinal direction of the bridge on static parameters of bridge is presented in Table 10. It is clear in this table, no significant developments in bending moments as function of the stiffness can be seen. Even the percent of moment contribution between girder and main cable has no noticeable change (Fig. 22). Only the frequency of the first torsional mode increases. Torsional mode of the

Table 9. Influence of sag to span ratio on bridge behaviour

f_1/L_1	N (kN)	H (kN)	R_z (kN)	$\delta_{main\ span}$ (mm)	δ_{pylon} (mm)	$M_{Y\ totoal}$ (kN-m)	$M_{Y\ support}$ (kN-m)	1^{st} *bending freq.* (Hz)	2^{nd} *bending freq.* (Hz)	1^{st} *torsional freq.* (Hz)	2^{nd} *torsional freq.* (Hz)
1/5*	32420	16542	6134	361	91	152065	193096	0.74	1.46	5.20	4.19
1/6	35545	18268	5739	400	83	186776	235639	0.71	1.47	5.82	4.74
1/7	37633	19491	5280	437	77	221178	277931	0.68	1.47	6.18	5.18
1/8	38934	20326	4808	471	73	253476	317643	0.66	1.47	6.40	5.52
1/9	39665	20871	4352	500	68	282937	353788	0.64	1.47	6.51	5.80

*Properties of reference design

Table 10. Influence of sag pylon stiffness on bridge behaviour

I_{pylon} (mm_4)	N (kN)	H (kN)	R_z (kN)	$\delta_{main\ span}$ (mm)	δ_{pylon} (mm)	$M_{Y\ totoal}$ (kN-m)	$M_{Y\ support}$ (kN-m)	1^{st} *bending freq.* (Hz)	2^{nd} *bending freq.* (Hz)	1^{st} *torsional freq.* (Hz)	2^{nd} *torsional freq.* (Hz)
0.238	32624	16428	6295	366	94	155668	196633	0.73	1.46	4.95	4.06
0.321	32558	16474	6240	364	93	154225	195172	0.73	1.46	5.1	4.12
0.419	32474	16519	6172	362	92	152780	193771	0.74	1.46	5.18	4.17
0.474*	32420	16542	6134	361	91	152065	193096	0.74	1.46	5.2	4.19
0.664	32232	16608	6003	357	89	149845	191088	0.74	1.47	5.3	4.25
0.812	32082	16653	5903	354	87	148354	189786	0.75	1.47	5.32	4.28

*Properties of reference design

girder exhibits with longitudinal motion of the pylon, therefore a stiffer pylon has a positive effect on the torsional stiffness of the bridge. Hence, in Table 10, it can be seen that the pylon offers more resistance against a torsional mode of the girder.

6. Increasing Span Length

One of the main concerns with an increasing span is the design of the stiffening girder. The axial compressive force, bending moments and second order effects are determining factors in the design of the stiffening girder. Other important aspect is the erection phase of a self-anchored suspension bridge. The distance between the temporary supports can easily govern the girder design regarding the required bending stiffness. Much attention is needed for the design of a stiffening girder to meet the different requirements in the erection phase of the bridge. Therefore, the scope is trying to find a limit in span possibilities related to mechanical required properties of the stiffening girder. The considered required properties of the stiffening girder will be the bending stiffness (EI_{girder}) and the cross sectional area (A_{box}).

To be able to increase the span length in the reference model and analyzing the effect on required mechanical properties for the stiffening girder, all other dimensional and mechanical properties should stay fixed. Only then, a fair comparison of the results is allowed. Increasing the span in the reference model is done by means of several scaling factors for cable sag, side span, hanger distance, cable diameter, girder slenderness and pylon stiffness, which are fixed in the following ratio:

- Sag to span ratio $f_1/L_1 = 1/5$; This ratio determines the horizontal component of the cable force and therefore the compression force in the stiffening girder. Keeping this ratio fixed enables to discover the influence of the increment of the compression force on the behaviour of the stiffening girder.
- Main span to side span ratio $L_1/L_2 = 2.4$; This ratio is kept fixed to rule out any influence of main span to side span ratio on the behaviour of the stiffening girder.
- Diameter of main cable to main span ratio $D/L_1 = 210/150 = 1.4$; Theory shows that an increment of the span length gives an exponential increase of the horizontal cable component ($H_{main\ cable}$). To maintain the same level of stress in the cable, the cross sectional area (A_{Cable}) should therefore be increased. Cross sectional area of a circular cable is proportional to the square of the diameter. Therefore, an increment of the span length gives a linear increase of cable diameter (D). Self-weight of the cable per unit of length remains constant under fixed sag to span ratio, when diameter is unchanged. A fixed diameter to span ratio keeps the level of stresses due to self-weight effects constant.
- Hanger distance to main span ratio = 1/24; This ratio is kept fixed to rule out any influence of the hanger distance on the behaviour of the stiffening girder. The cross sectional area of the hangers is linearly scaled with an increasing core to cores distance of the hangers.
- Deck height to main span ratio (deck slenderness) $h/L_1 = 1/95$
- The main span length is increased with step sizes of 50 m up to 500 m. For each step, an evaluation is made on static strength, stiffness and stability criteria.
- The vertical clearance under the bridge deck is kept fixed to 15 m. The pylon height under the bridge deck is therefore also fixed on 15m.
- The pylon height increases with a larger span because the sag to span ratio is kept fixed. An increasing pylon height requires more stiffness. Therefore, the longitudinal stiffness is scaled. The ratio $L^3/I_{y\ pylon}$ is kept fixed to have comparable stiffness of the pylon in the longitudinal direction of the bridge for increasing span lengths.

Increasing the span length of the bridge will cause several effects on static strength and stiffness. Several key parameters are monitored to analyse these effects and to verify if the before mentioned scaling assumptions are applicable and valid. The key parameters are:

- Stresses in cable, girder and pylon
- Second order effects
- Deformation of girder and pylon
- Vertical reaction force at end support and normal force in the deck of the bridge
- Materials of cable, deck and pylon

Table 11. Main results of increasing span

L (m)	N_{deck} (kN)	H_{cable} (kN)	R_z (kN)	$\delta_{main\ span}$ (mm)	δ_{pylon} (mm)	$M_{y;main}$ (kN-m)	$M_{y;support}$ (kN-m)	1^{st} *bending freq.* (Hz)	1^{st} *torsional freq.* (Hz)	1^{st} *transverse freq.* (Hz)
150	37682	19136	7679	336	87	83959	111176	0.72	4.43	5.21
200	54028	27361	11306	410	108	100200	139068	0.60	3.40	3.15
250	70944	35857	15048	468	127	115276	168634	0.52	2.81	2.10
300	88679	44773	18966	519	144	128073	198965	0.46	2.35	1.50
350	107413	54178	23091	567	161	139339	232275	0.40	2.00	1.12
400	127275	64153	27453	613	178	150087	270473	0.36	1.75	0.87
450	148451	74784	32089	660	196	159235	314120	0.32	1.53	0.70
500	171108	86155	37037	706	214	167839	365235	0.29	1.36	0.57

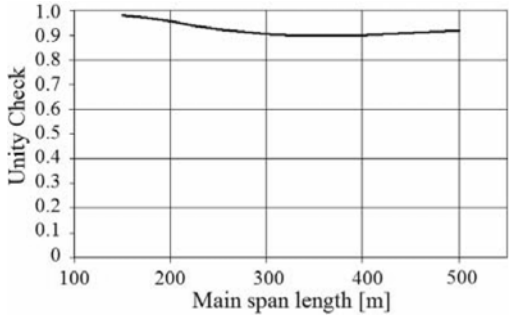

Figure 24. Development on Unity Check deflection of main span.

Table 12. Girder properties for the considered span lengths

Main span length (m)	Slenderness λ	Girder height (m)	A_{total} (m)	I_y (m^4)	I_z (m^4)	I_t (m^4)
150	1/95	1.6	2.18	1.26	241	3.15
200	1/95	2.1	2.2	2.17	246	5.33
250	1/95	2.63	2.22	3.4	251	8.2
300	1/95	3.16	2.23	4.9	256	11.62
350	1/95	3.68	2.25	6.68	261	15.52
400	1/95	4.21	2.26	8.78	266	20.07
450	1/95	4.74	2.28	11.1	271	24.77
500	1/95	5.26	2.29	13.77	276	30.09

7. Effects of Increasing the Span by Scaling

The span length of the optimized bridge model is increased to 500 m and bridge components are scaled. Table 11 shows the main results of member forces and deflections caused by self-weight, permanent loads and traffic over the full length of the bridge.

Horizontal equilibrium shows that $2 \times H_{main\ cable} = N$, but Table 11 shows a little deviation caused by the fact a very small part of the horizontal component of the cable force $H_{main\ cable}$ is resist as bending in the pylon's base.

A quick stiffness check ($\delta_{max\ allowable} = L_1/350$) reveals that the scaled bridges up to 500m performs very constant regarding the maximum allowable deflection of the main span. Fig. 24 shows the constant performance regarding deflection of the main span; the unity check varies between 0.9-0.98. In this case, the unity check regarding stiffness is determined by:

$$UC = \delta_{main\ span}/\delta_{max\ allowable} \quad (9)$$

So on stiffness criteria, increasing the main span length up to 500 m by means of the scaling factors, satisfies and displays a constant performance.

8. Results of Increasing Span

The scaling of the bridge model up to 500 m proved very constant regarding the global stiffness of the bridge, therefore, no adjustments are in made according to the previous mentioned scaling assumptions. Hence, a comparison with some analyses is made regarding the developments on all other important design criteria and design aspects with an increasing main span.

This section will briefly discuss these design criteria and mention the critical issues, which require consideration in the design process of a self-anchored suspension bridge.

8.1. Static behaviour

To give a total view on static behaviour, the development of the level of the stresses in the box girder, the main cable, the hangers and pylon are investigated.

A fixed girder slenderness of $\lambda = 1/95$ is chosen for several span lengths. The mechanical properties of the box girder for each span length are given in Table 12.

In order to determine cross sectional requirements (e.g. plate thicknesses) of a box girder in the design process, the compressive and tensile stresses that are present in the top and bottom flanges are calculated. The stresses are caused by the global bending moment in the girder and compressive force in the girder by the main cable. The actual stresses in the top and bottom flanges are presented in Figures 25 and 26.

According to Fig. 25, stresses in the compression flanges of the side and main span of the girder have a nearly constant development. This indicates that the chosen girder dimensions for each considered span length are properly chosen. The significant decrease of the

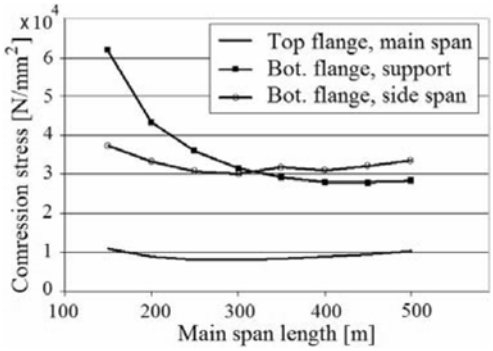

Figure 25. Stresses in compression flanges.

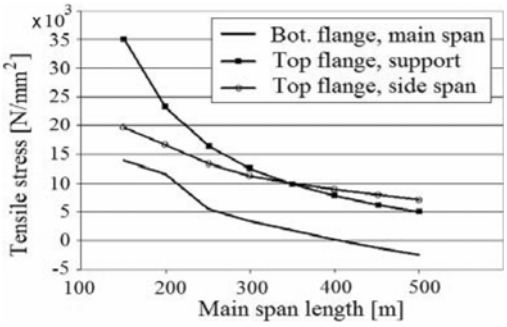

Figure 26. Stresses in tensile flanges.

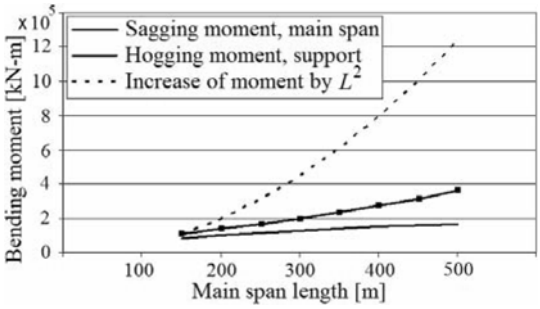

Figure 27. Development of the maximum bending moment in the girder.

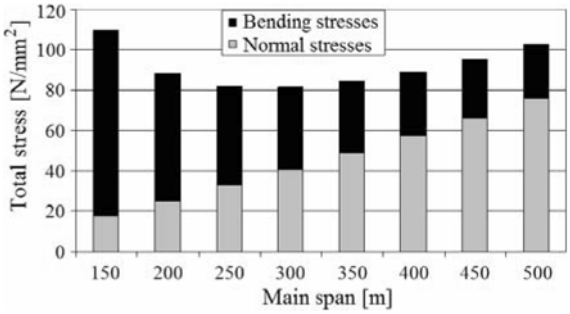

Figure 28. Contribution of the normal compressive stress in the top flange in the main span.

compression stress at the support location is caused by the fact that the hogging moment (but also the sagging moment at main span) does not increase that rapidly with an increase of the main span. In case of an unsupported main span, for instance a simply supported beam, an increase of the main span length (L_1) will result in an increase of the maximum sagging moment by L_2. The girder of a suspension bridge is continuously stiff supported by the hangers, so increasing the main span of the bridge with a length L_1 does not result in an increase of the global bending moments of L_2 but much less. In Fig. 27, the dotted line represents a development of the bending moment with an increase by L_2 and the actual development of the maximum bending moments in the continuous spring supported deck in main span of the bridge.

Fig. 26 shows that also the stresses in the tensile flanges of the box girder display an overall decrease on all locations. Besides the confined development of the bending moments other causes for this decrease in tensile stresses in the flanges of the box girder are:

- For each span the same slenderness $\lambda = 1/95$ of the box girder is chosen. Therefore, the height of the box girder is with each increment of the main span linearly increased. Section properties like the moment of inertia and the section modulus increase also. The section modulus of elasticity increases linearly but the bending moments do not increase that significant, so the bending stresses decrease with an increasing span length (Fig. 26).
- With an increasing span, the stress caused by the compressive force in the girder becomes dominant over the bending stresses (Fig. 28). Therefore, a decreasing develop-ment is visible in tensile stresses presented in Fig 26. Compressive stresses become dominant in the cross section of the box girder for an increasing span.

Even a point can be reached where compression stresses can occur in the normally tensile bottom flange of the box girder in the main span (Fig. 26), at a main span of 400m. This will have effect on the design of the bottom flange in the mid of the main span, if compression stresses occur also here, then local instabilities have to be checked and it is likely that more stiffeners have to be applied (as is the case for the compressive bottom flange at support location at the pylon).

Overall, for an increasing span length, stress levels in the box girder are of manageable levels. Local additional plate thicknesses and stiffeners are required for some locations depending on the span length.

The influences of diameters of main cable and hangers on static behaviour of the bridge have also been checked. The applied main cable and hanger properties for each span length are given in Table 13.

With an increasing span, the level of the maximum tensile stress in hangers stays approximately on the same level but for the main cable, a decreasing stress level is clearly visible in Fig. 29. This result indicates that stiffness is the governing design criteria over strength criteria for suspension bridges, even for relative short

Table 13. Main cable and hangers properties

Main span Lengt (m)	D_{cable} (mm)	A_{cable} (mm^2)	D_{hanger} (mm)	A_{hanger} (mm^2)
150	210	34636	55	2376
200	280	61575	64	3217
250	350	96211	71	3959
300	420	138544	78	4778
350	490	188574	84	5542
400	560	246301	90	6362
450	630	311725	95	7088
500	700	384845	100	7854

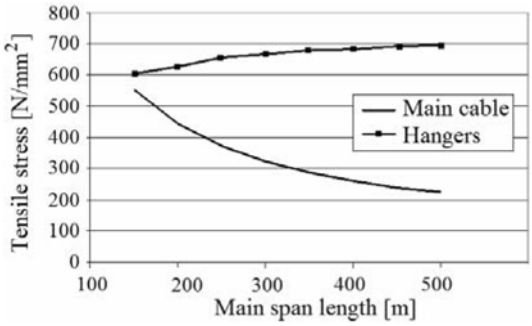

Figure 29. Stress level in main cable and hangers.

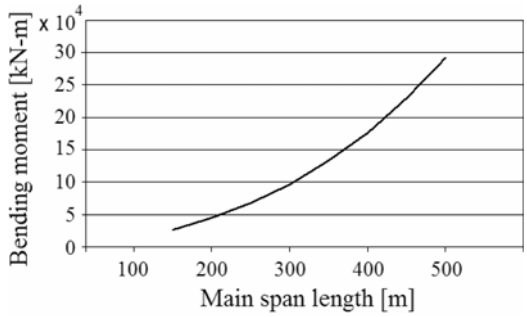

Figure 30. Bending moment at pylon base.

spans up to 500 m. The amount of material required for the main cable becomes with an increasing span length less efficient on strength; the additional required main cable area is needed to satisfy stiffness criteria.

Without any provisions, an increasing main span would increase the bending moments at the pylon drastically and can therefore become critical (Fig. 30).

8.2. Buckling stability of the stiffening girder

With assistance of the parameter study, for each increment of the main span, with step sizes of 50m, the buckling force is determined. An additional force of ΔF = 400000 kN has been applied to deck element in order to obtain visible second order effect in the deflection of the stiffening girder. Fig. 31 presents the results for buckling force calculation for each considered span length up to 500 m for a loading combination including self-weight, permanent loading, traffic load over the full length of the bridge and pre-tensioning of the main cable.

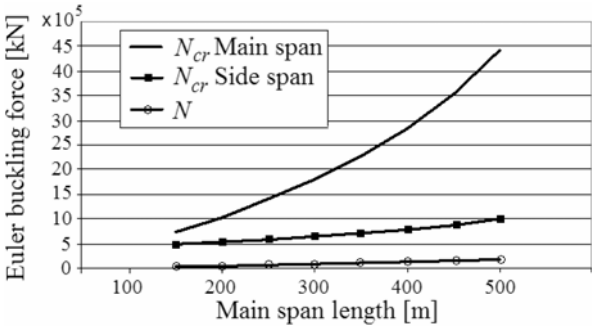

Figure 31. Development of the deck Euler buckling force as a function of an increasing main span.

As it is obvious in Fig. 31, the buckling force N_{cr} for the side span is well below the N_{cr} of the main span, even for an increasing main span up to 500 m.

The reason for the increased Euler buckling force for an increasing span is the fact that, the height of the box girder is linearly increased with the main span. This will increase the moment inertia more than quadratic, and so the bending stiffness is increased with the same proportion.

If the above presented graph is expressed in the so-called *n*-value, then it becomes visible that buckling is getting more and more critical with an increasing span. The *n*-value defined as:

$$n_{side\ span} = \frac{N_{cr,side\ span}}{N} \tag{10}$$

$$n_{main\ span} = \frac{N_{cr,main\ span}}{N} \tag{11}$$

The *n*-value for each considered span lengths are given in Table 14. The Eurocode3 gives guidance with respect to the *n*-value. Eurocode NEN-EN 1993-1-1 part 6.3.1.2 states when N/N_{cr} 0.04 the buckling effects may be ignored and only cross sectional checks. The *n*-values in Table 14 do not satisfy this term, so the geometrical non-linearity should be taken into account.

For the main span, the buckling mode is downward and

Table 14. The *n*-values for main and side span

Main span length (m)	*n*-value main span	Side span length (m)	*n*-value side span
150	19.8	63	12.9
200	19.2	83	9.9
250	19.7	104	8.3
300	20.4	125	7.3
350	21.2	146	6.6
400	22.3	167	6.2
450	23.8	188	5.9
500	25.8	208	5.8

would therefore encounters upward resistance by the hangers while the buckling of the side span is an upward buckling mode. The upward buckling of the side span occurs at a much lower buckling force (N_{cr}) and is decisive over buckling of the main span. The buckling stability of the side span girder becomes more and more a critical design issue with an increasing span up to 500 metres. The so-called *n*-values given in Table 14 indicate that the consequences on geometrical non-linearity have become more evident with an increasing main span.

The given approach to research the buckling stability of the girder presented in this study has shown that buckling of the main span is not decisive. In this approach, a stiffening girder is chosen with the same slenderness along the complete length of the bridge. With *n*-values of 20 or more, regarding buckling of the main span, a much more slender girder could be chosen for the main span. This can be of great contribution to the reduction of material use.

Research to the buckling phenomena of the side span has shows that with an increasing span, the resistance against buckling of the side span reduces. Up to a main span length of 500 m, buckling of the stiffening girder should be analyzed in the design process but it is possible to reach such a span length. Thus, with respect to the buckling stability of the stiffening girder, a self-anchored suspension bridge is possible up to a main span of 500 and maybe even beyond that. Assuming a limitation for the girder slenderness of about $\lambda = 1/100$ regarding the buckling stability of the deck is point of discussion.

8.3. Frequency behaviour

A good indication for the resistance against flutter is the development of the ratio between the torsional and bending frequency. With an increasing main span both bending and torsional frequency decrease significantly but the ratio between these frequencies stay well above the general accepted level of 2 (Table 15). When this ratio is above two then the structure should have enough resistance against flutter instability (Chen and Duan, 2000). A decreasing ratio between the bending and torsional frequency indicates that the bridge structure becomes more sensitive for flutter.

The natural frequencies obtained in this research give room for the possibility of choosing a more slender deck than $\lambda = 1/95$ that is chosen in this research.

8.4. Reaction forces

The reaction forces at the end support have to be resisted with vertical anchorage. The horizontal reaction force will be resisted in the deck. In the case that side spans have no traffic load; the vertical reaction force at end supports has the maximum value. Therefore, the load combination including self-weight, permanent loading, cable pre-tensioning and traffic load over the main span is used to present the influence of increasing span on reaction forces.

Table 15. Frequency ratio for each span length

Main span length (m)	1st *bending freq.* (Hz)	1st *torsinal freq.* (Hz)	*torsional freq. / bending freq.*
150	0.72	4.43	6.2
200	0.6	3.4	5.7
250	0.52	2.81	5.4
300*	0.46	2.35	5.1
350	0.4	2	5.0
400	0.36	1.75	4.9
450	0.32	1.53	4.8
500	0.29	1.36	4.7

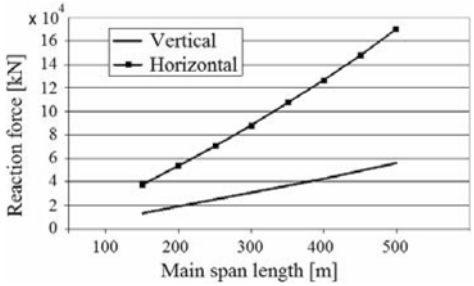

Figure 32. Reaction forces at the end supports.

The critical issue will be the horizontal anchorage of the main cable (Fig. 32). Due to the complex nature of the horizontal anchorage of the main cable, it requires much attention. For an increasing main span, the horizontal cable force increases rapidly and is has enormous consequences for the horizontal anchorage. The introduction of the horizontal cable force requires many provisions like anchor shoes, plate stiffeners. With an increasing main, the main cable diameter increases and contains more strands to be anchored.

8.5. Material use

To give an estimate of amount of steel used in the main bridge components like deck, pylon, main cable and hangers, Figures 33 and 34 are presented. For each span up to 500 m, the amount of steel has been calculated and a differentiation is made to the steel use of each bridge components. For an increasing main span, the required amount of steel grows almost linearly (Fig. 33).

By far the biggest part of material use is required for the stiffening girder. For a bridge model with a main span up to 500 m, the stiffening girder takes at least 70 percent of the total material use. Moreover, for an increasing main span the contribution of the material use in the main cable becomes significant. The main cables and hangers can take up to 25 percent of the material use. So the biggest cost reduction can be achieved by saving material in the stiffening girder. Reducing the slenderness of the girder in the main span, and increasing the axial stiffness the cable in order to reduce the bending moment in the girder will be helpful for this goal.

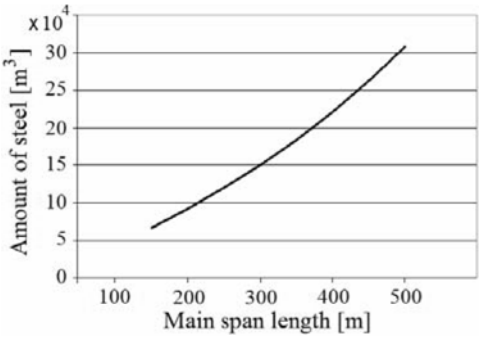

Figure 33. Total amount of steel.

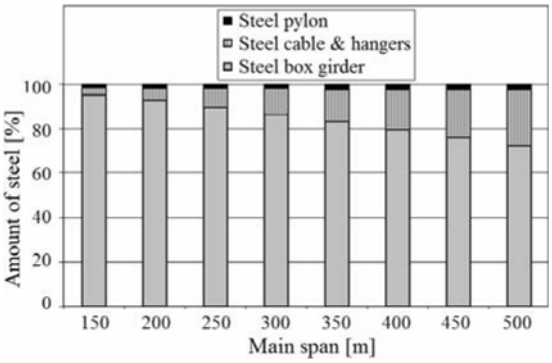

Figure 34. Steel use per category.

9. Conclusions

From this parametric study of static behaviour of self-anchored suspension bridges, the following conclusions can be drawn:

(1) The buckling stability of the girder requires attention in the design process of a self-anchored suspension bridge. However, a girder with a slenderness around $\lambda = 1/100$ is expected to have enough resistance against buckling. Extrapolating this graph for even more slender girders, meaning a higher slenderness $\lambda = 1/100...1/150$ and further, a limitation is expected with respect to the buckling resistance. These slenderness of stiffening girders in existing self-anchored suspension bridges is limited to around $\lambda = 1/100$ (e.g. Konohana bridge, Japan). Compare this to the applied stiffening girders in conventional suspension bridges where no buckling risk of the girder is present, here girder slenderness of $\lambda = 1/200 - 1/300$ are common.

(2) Regarding the force distribution and deflection, it is favourable to consider a stiff main cable, to increase the global stiffness of the bridge and to reduce the maximum bending moment in the girder, and also increase sag to span ratio, to reduce the normal force in the deck and the maximum bending moment in the deck. A high sag ratio showed to be favourable for the bending moment distribution, deflections of the deck and the normal force in the deck. Therefore, a sag ratio of 1/5 will be a good choice for design.

(3) It is important to consider the level of frequencies. The ratio between the first bending and the first torsional frequency illustrates the risk for flutter. A ratio close to 1.0 is not desirable; in general, a ratio of 2.0 or more is advisable. The results show that the ratios of the 1st bending to 1st torsional frequencies are in all cases well above 2. Therefore, in this case this criterion plays a secondary role.

(4) The results show that the influence of the pylon stiffness, in longitudinal direction of the bridge on the global behaviour, is negligible. So no changes are made in the mechanical properties of the pylon.

(5) The cable cross sectional area can be altered to meet static strength criteria of the cable and girder and the deflection criteria of the girder and pylon. The axial stiffness (EA) of the cable is an important parameter to influence the force distribution and stiffness of the bridge. Increasing (EA) of the cable increases the stiffness and reduces the bending moments in the girder significantly.

(6) An important aspect to influence the force distribution in a self-anchored suspension bridge is the ratio between the deck bending stiffness (EI_{girder}) and the cable axial stiffness (EA_{cable}). It is more profitable to increase cable axial stiffness in order to increase the stiffness of the bridge and to reduce the bending moments in the stiffening girder. Designing and dimensioning structural bridge members under bending is always less effective and more material consuming than that of members under tensile loading, such as the main cable. The stiffness criteria, expressed in allowable deflections, are easily met by choosing the proper dimension for the main cable. For a bridge span length up to 500m, global stiffness is not a critical design issue.

(7) There is a difference in the buckling force (N_{cr}) of the side and main span. Based on the assumptions in this research, buckling of the girder in the side span is decisive. A chosen girder slenderness of $\lambda = 1/95$ is sufficient to resist buckling. Even for the main span, a more slender girder is possible because the n-value is around 20-25 for a span length up to 500 m. A slender girder can be of great contribution of cost reduction, since the girder takes at least 70% of the total steel use in the bridge.

(8) Required slenderness of the box girder is mainly dominated by the erection method on temporary supports and not so much the buckling stability. Depending on the circumstances during erection the slenderness of the box girder is can be even more slender than $\lambda = 1/95$.

(9) In this case sag over span ratio has been chosen of 1/5 in order to reduce the bending moments and normal force in the girder. Regarding the buckling stability of the girder, which is sufficient with a girder slenderness of $\lambda = 1/95$, a smaller sag ratio can be considered which increases the normal force the deck. Decreasing the sag to span ratio contributes to the reduction of the main cable length and pylon height.

Notation

The following symbols are used in this paper:

β_m : equivalent moment factor, (according to table A.2 of EN-1993-1-1)
δ_1 : deflection determined by a first order analyses (linear)
δ_2 : deflection determined by a second order analyses (geometric non-linear)
$\delta_{main\ span}$: maximum vertical deflection of main span
$\delta_{max\ allowable}$: maximum allowable vertical deflection of main span
δ_{pylon} : deflection of top of pylon in long. Dir
ΔF : external additional force applied on girder
ΔM_Y : moment due to shift of the centroidal axis
λ : deck slenderness
σ : stress in cable
χ : reduction factors due to flexural buckling
A_{Cable} : main cable cross section
A_{total} : box girder cross section
c : bedding constant equal to the spring stiffness divided by the c.t.c. distance between the hangers
D : diameter of main cable
e : eccentricity of the resulting line load to the gravity centre of the box girder
E : modulus of Elasticity
f_1 : sag in main span
f_2 : sag in side span
f_y : Yield strength
F_{res} : resulting three axle loads
$H_{main\ cable}$: axial force in main cable
h : deck height
I_{Girder} : main girder moment of inertia about Y axis
I_t : main girder torsional moment of inertia
I_y : main girder moment of inertia about Y axis
I_z : main girder moment of inertia about Z axis
I_{Pylon} : pylon moment of inertia about lateral axis
k : spring stiffness
l : horizontal span of cable
L_1 : main span length
L_2 : side span length
$M_{Y,deck}$: design value of maximum moment about the Y axis
$M_{Y,main}$: main span maximum moment about Y axis
$M_{Y,support}$: side span maximum moment about Y axis
$M_{Y,total}$: total bending moment in main span
n : amplification determined from deflection in the first order and second order analysis of the bridge model
N : design value of compression force in deck
N_{cr} : elastic critical force for the relevant buckling mode based on the gross cross sectional properties
N_{deck} : normal force in deck
$q_{res,traffic}$: resulting traffic line load
R_z : vertical reaction force at end support
UC : ratio of maximum deflection in main span to maximum allowable deflection
w : unit weight of cable

References

Chen, W. and Duan, L. (2000). "Bridge Engineering Handbook", CRC Press, New York, N.Y., USA

Clemente, P. Nicolosi, G. and Raithel, A. (2000), "Preliminary design of very long-span suspension bridges", Engineering structures, Vol. 22, pp. 1699-1706

Engesser, F. (1889). "Uber die Knickfestigkeit gerader Stäbe." Zeitschrift für Architektur und Ingenieurwesen, 35(4), pp. 455-562

Ernst, H. J. (1965). "Der E-Modul von Seilen unter Berücksichtigung des Durchhängens." Bauingenieur, 40, pp. 52-55

European Prestandard 1993-1-11, (2003). Eurocode 3-Design of Steel Structures, Brussels, Europe

Gasparini, D. and Gautam. V. "Geometrically Nonlinear Static behaviour of Cable Structures", Journal of Structural Engineering, October 2002, pp. 1317-1329

Gimsing, N.J., Cable supported Bridges, Wiley&Sons, 1998

Kim, H.K., Lee, M.J. and Chang, S.P. (2002), "Non-linear shape-finding analysis of a self-anchored suspension bridge", Engineering Structures, Vol. 24, pp. 1547–1559

SCIA ESA-PT, (2006). User's manual, version 6.0.185, SCIA Scientific software, EU

Ren, W. "Roebling suspension bridge. 1:Finite element model and free vibration response", Journal of Bridge Engineering, March/April 2004, pp 110-118

Ulstrup, C. C. (1993). "Rating and preliminary analysis of suspension bridges." Journal of Structural Engineering, Elsevier, 119(9), pp. 2653-2679

Van Goolen, D. (2007). "Self-anchored suspension bridges." M.Sc. thesis, Technical University of Delft, The Netherland.